Journal of Sol-Gel Science and Technology (2025) 114:916–933
https://doi.org/10.1007/s10971-025-06749-x

ORIGINAL PAPER

# Enhancing textile properties using nanotechnology and 3D printing process

Rosa Taurino[1,2] · Maria Cannio[3] · Stefano Martinuzzi[2] · Stefano Caporali[1,2] · Francesca Borgioli[1,2] · Emanuele Galvanetto[1,2] · Dino Boccaccini[3,4]

Received: 31 January 2025 / Accepted: 30 March 2025 / Published online: 12 April 2025


## Abstract

This study explores the application of chitosan-based sol–gel coatings on textile fabrics to achieve multifunctional surfaces with enhanced hydrophobicity and stain resistance. Sol–gel solutions were prepared using chitosan, vinyltrimethoxysilane (VTMS), and tetraethyl orthosilicate (TEOS), with concentrations of 2 wt% and 5 wt%. Additionally, the effect of UV curing was investigated. The coatings were applied to pure cotton and synthetic polyester fabrics using dip-coating and digital deposition techniques. To ensure uniform deposition in the printing process, key solution properties including viscosity, density, and surface tension were optimized. The chemical and physical characteristics of the coatings were analyzed through FTIR and DSC, while SEM imaging, color measurements, water contact angle assessments, and stain and abrasion resistance tests were conducted to evaluate their impact on textile properties. The results demonstrated significant improvements in hydrophobicity, with water contact angles reaching up to 120° compared to non-functionalized textiles. The coatings also enhanced stain and abrasion resistance, exhibiting low friction coefficients and minimal degradation after multiple washing cycles. In the final phase of the study, we investigated the integration of the sol–gel technique with 3D inkjet printing to create films with a more uniform structure while preserving the hydrophobic properties of the coatings. These findings highlight the feasibility of using chitosan-based sol–gel solutions for textile functionalization, offering promising results for both conventional and digital application methods. This approach paves the way for advanced, eco-friendly, and multifunctional textile coatings.

## Graphical Abstract

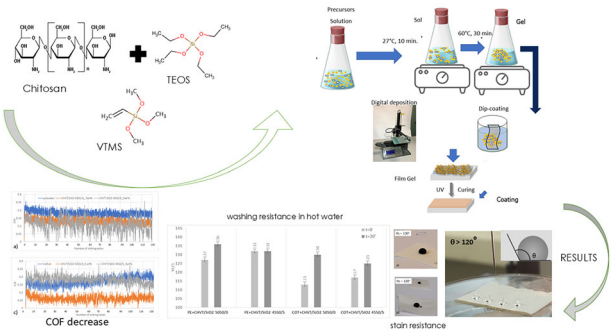


✉ Rosa Taurino
rosa.taurino@unifi.it

[1] Department of Industrial Engineering, University of Florence, Via di Santa Marta 3, Firenze 50139, Italy

[2] National Interuniversity Consortium of Materials Science and Technology (INSTM), Via Giusti 9, Firenze 50121, Italy

[3] Resoh Solutions SRL, Via Pietro Guardini 476/N, 41124 Modena, Italy

[4] Dipartimento di Ingegneria "Enzo Ferrari", Università degli studi di Modena e Reggio Emilia, Via Vivarelli 10, 41125 Modena, Italy

**Keywords** Sol–gel process · Chitosan · Ecofriendly coatings · Textile fabrics · 3D printing process

**Highlights**

- Sol–gel process nanotechnology for textile fabrics.
- Chitosan-based hybrid coatings as potential alternative to hazardous chemicals.
- Textile fabrics with multifunction properties have been obtained.
- Implementation of the sol–gel technique in combination with 3D printing technology.

## 1 Introduction

The functionalization of textiles generally refers to all processes used to provide fabrics with multi-functional characteristics. Among the most promising and innovative methods, the sol–gel process stands out as a cutting-edge approach in nanotechnology and materials science for synthesizing nanostructured materials [1]. Unlike conventional textile treatments the sol–gel technique facilities the development of multifunctional properties in a single step, enabling the production of coatings with novel characteristics or the integration of various functions into a single fabric. This process offers several advantages, including reduced chemical usage low temperatures operations, and one-step application, making it an environmentally ecofriendly approach that significantly minimizes both water and energy consumption [2, 3].

For several years, sol–gel techniques have gained significant attention in the textile sector for their ability to impart multifunctional properties to fabrics [4]. By leveraging nanotechnology, textile materials can be engineered to exhibit specific functionalities such as hydrophobicity, antibacterial properties, conductivity, antistatic properties, UV and abrasion resistance, without compromising their breathability and texture. The sol–gel process, widely used in the chemical finishing of textiles, often involves a pad-dry-cure method. During this process, a dense nanocomposite polymer film, approximately 10-nm thick, is formed on the surface of the fibers preserving the comfort, flexibility, or the light weight nature of the fabrics. Additionally, the M–OH groups of the sol–gel precursors can react with the fiber surface, forming hydrogen or covalent bonds depending on the substrate, ensuring strong adhesion and durability [5, 6]. Various textile materials including cotton, silk or polyester are ideal substrates for integrating functional nanomaterials [7]. Multiple approaches have been employed to impart hydrophobic and multifunctional properties to textile using sol–gel technique and nanosol coatings. For istance, Bae et al. [5] synthesized silica ($SiO_2$) nanoparticles (NPs) through a sol–gel process combined with water-repellent agents to enhance cotton fabrics' water repellency. In their approach, they used a perfluorooctylatedquaternary ammonium silane coupling agent which significantly improved both hydrophobicity and oil repellency, demonstrating the potential of sol–gel techniques for advanced textile finishing.

Sol−gel coatings based on alkoxysilanes modified with alkyl chains and hydrophilic compounds, such as amino-functionalized alkoxysilanes have been used as surface treatments to impart both antistatic properties and hydrophobic properties to textiles [8, 9]. Moreover, $TiO_2$-based sol–gel coatings have been developed to provide UV protection [10, 11]. In another example, Gao et al. [8] demonstrated a method to achieve highly hydrophobic surfaces on cotton and polyester fabrics. Their approach involved treating the fabrics with silica nanoparticles synthesized through the hydrolysis and subsequent condensation of tetraethoxysilane under alkaline conditions followed by hydrophobization using hydrolyzed hexadecyltrimethoxysilane (HDTMS). This treatment resulted in textiles with excellent water repellency and durable hydrophobic properties.

The potential of sol–gel hybrid coatings for the functionalization of silk fabrics, was evaluated by the de Ferri et al. [12] focusing on improving their abrasion resistance and stain-repellency of silk fabrics. To achieve this, various organic-inorganic hybrids coatings-based tetra-ethyl-orthosilicate (TEOS) and Si-alkoxides functionalized with either alkyl chains or fluorinated groups were developed. Then, sol–gel technology can be applied to textiles to develop various functional finishes with antibacterial [13, 14], water repellent [15–17], oil/water separations [18, 19], flame-retardant [20, 21] multi-functional [22, 23], ultraviolet (UV) protection [24] and abrasion resistance properties [25].

Despite the significant advancements in sol–gel textile functionalization, concerns regarding the environmental impact of fluorinated substances and the high cost of certain materials have driven research toward alternative, sustainable solutions [2, 3], such as chitosan. Chitosan, a bioactive and biodegradable polymer derived from natural waste, is an excellent candidate for the developing multifunctional coatings for textile due to its non-toxicity and ease of modification. Several studies have demonstrated that it is possible to obtain chitosan-based films using the sol–gel process to impart antistatic, hydrophilic or hydrophobic properties [26–29].

**Table 1** List of the different coatings' compositions

| Sample ID | Chitosan (wt.%) | VTMS (wt.%) | TEOS(wt.%) | Solution concentration (wt.%) |
|---|---|---|---|---|
| Ch/$SiO_2$ 100/0_5wt% | 100 | 0 | 0 | 5 |
| ChVT/$SiO_2$ 5050/0_5wt% | 50 | 50 | 0 | 5 |
| ChVT/$SiO_2$ 4550/5_5wt% | 45 | 50 | 5 | 5 |
| ChVT/$SiO_2$ 5050/0_2wt% | 50 | 50 | 0 | 2 |
| ChVT$SiO_2$ 4550/5_2wt% | 45 | 50 | 5 | 2 |

Nevertheless, one of the main drawbacks of applying chitosan to textiles is the low water resistance of the biopolymer, which negatively affects its wash fastness. To address this issue, thermal treatment or the use cross-linking agents is necessary to achieve strong bonding between chitosan and textile substrates [30]. However, since thermal curing involves energy consumption and may lead to textile degradation, UV irradiation offers a cost-effective and eco-friendly alternative for producing chitosan-based coatings on textile fabrics. For instance, Ferrero et al. [31] developed a UV-curable chitosan-based textile finish to provide antimicrobial properties. In their study, various types of textile fabrics were impregnated with an acidic solution of chitosan, containing a photoinitiator, followed by curing at room temperature under UV light.

Unlike previous studies, our research pioneers the development of novel hybrid sol–gel coatings by integrating chitosan with vinyltrimethoxysilane (VTMS) as organic and inorganic precursors, followed by UV curing after application to the fabrics. VTMS, which contains silicon-oxygen bonds, was used alongside chitosan as a finishing agent. To explore the potential of these coatings, two different sol–gel systems with varying concentrations were designed: the first composed of chitosan and VTMS, and the second incorporating tetraethoxysilane (TEOS) to evaluate the effect of silica on the coating properties. Surface analyses and functional assessments of the treated textiles were conducted to determine the coatings' effectiveness. Analyses of the textiles' surfaces and the determination of changes in their properties caused by the functionalization were performed.

In addition, this study explored the feasibility of applying sol–gel solutions onto textile fabrics using 3D inkjet printing. As highlighted in several studies [32–37], achieving optimal printing performance requires careful control of key parameters such as viscosity, density, surface tension to prevent/avoid splashing phenomena. Cotton and synthetic polyester fabrics were chosen as textile substrates due to their widespread use in various applications, ranging from personal apparel and industrial coverings to medical supplies and healthcare products [38–40].

By integrating nanotechnology with sustainable processing techniques, this study presents a novel and eco-friendly alternative to perfluorinated chemicals in textile finishing. The findings pave the way for advanced, multifunctional, and environmentally sustainable textile coatings, with potential applications in healthcare and protective textiles.

## 2 Experimental section

### 2.1 Materials and preparation

Chitosan (Oxford, Vitality) with viscosity of 7-8 mP*s, degree of deacetylation ≥75%, glacial acetic acid (Alfa Aesar >99.9%), was used as received without further purification.

The degree of polymerization (DP) of the chitosan used in this study was estimated based on its intrinsic viscosity, following empirical correlations available in the literature. The chitosan employed (Oxford, Vitality) has a viscosity of 7–8 cps and a degree of deacetylation ≥75%. The weight-average molecular weight (Mw) was estimated using the empirical equation:

$$M_w \approx 10^3(\eta)^{0.76}$$

where η is the viscosity in mPa·s (cps) [41]. Applying this equation, the molecular weight of the chitosan was found to be in the range of 4388–4857 g/mol.

The degree of polymerization (DP) was then calculated as:

$$D_P = \frac{M_w}{M_{monomer}}$$

where $M_{monomer}$ is the molar mass of the repeating chitosan unit, approximately 161 g/mol, considering a degree of deacetylation ≥75%. Based on these calculations, the estimated DP of the chitosan used in this study is in the range of 27–30.

Vinyltrimethoxysilane (98% VTMS, Aldrich) was used as coupling agent and Tetraethyl orthosilicate (TEOS, Sigma Aldrich >99.9%) was used as silica precursor and

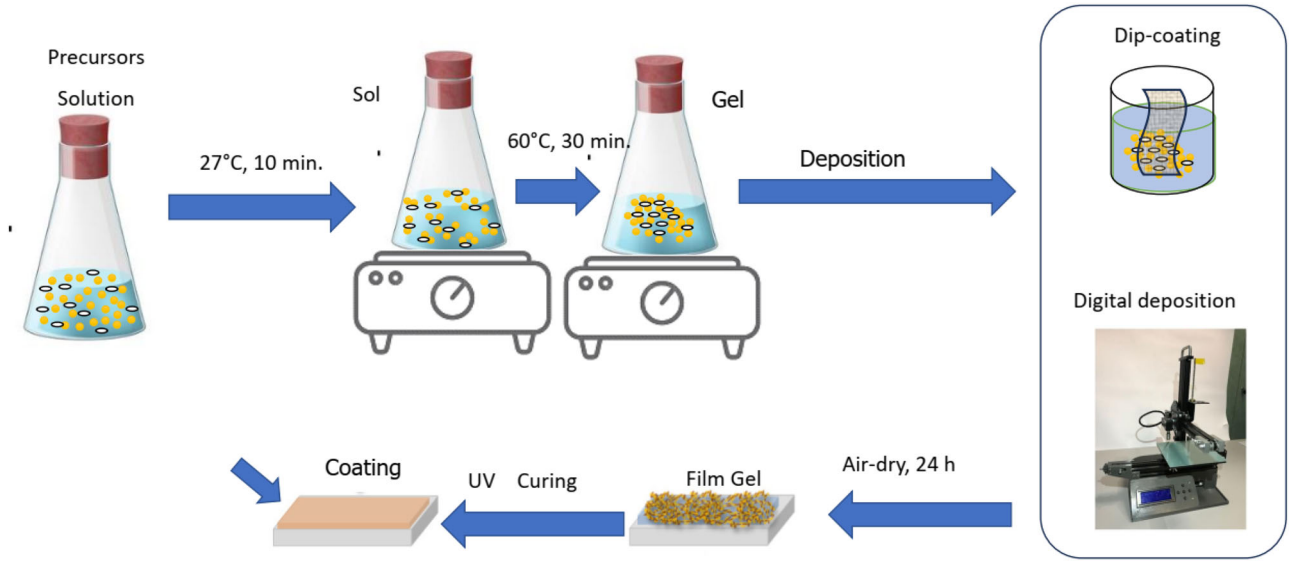


**Fig. 1** Schematic representation of the preparation procedure

ethanol (95 wt.% Sigma Aldrich) was used as received without further purification.

Solution concentration of 5 wt.% and 2 wt.% were used. 2-Hydroxy-2-methylphenylpropane-1-one (Darocur 1173, Ciba Specialty Chemcal) was used as photoinitiator. The photoinititor was added to the solution in the amount of 2 wt.%. The preparation conditions for each system are detailed in Table 1.

As illustrated in Fig. 1, the systems were prepared by mixing precursor solutions at 27 °C for 10 min, followed by vigorous stirring at 60 °C for 30 min to promote hydrolysis and condensation reactions. The relative humidity (RH) was about of 55–60%. The resulting solution was then applied using two different application technologies. For the dip-coating application, the substrates were immersed in the solution for 30 s, while for the digital application, 2 ml of solution was applied to a 3 cm × 3 cm surface. After a 24-h drying process at ambient temperature, the samples were UV-cured for 15 min using an Anycubic lamp with a light intensity of approximately 30 mW/cm². Fabrics treated were pure cotton and synthetic polyester fabrics previously washed but not subjected to any finishing process. To obtain free films for the DSC and FTIR characterizations, the solution was put onto silicon mould and after solvent evaporation the coatings was UV cured.

After successfully modifying the textile substrates, we explored the feasibility of applying the same solutions via digital deposition. To ensure compatibility with the printing process, we characterized the chemical and physical properties of the solutions such as density, viscosity, and surface tension since these parameters are critical for achieving homogeneous and uniform deposition, as reported in the literature [32–37]

## 2.2 Inkject printer

In the subsequent phase of this investigation, digital deposition techniques were utilized to assess the viability of employing a chitosan-based sol–gel solution within the context of digital deposition. The optimized sol–gel solutions were applied utilizing a custom-built micro-solenoid inkjet 3D printing apparatus. This apparatus was engineered through the modification of a commercially available Fused Deposition Modeling (FDM) 3D printer (Anycubic Kobra), wherein the original extruder was substituted with a system incorporating a direct-acting two-way micro-solenoid valve (type VA204-508, Staiger) characterized by a nozzle diameter of 250 µm, with ink being supplied through a hydraulic circuit sourced from a pressurized ink reservoir. A digital pressure sensor was employed to monitor and regulate the pressure within the reservoir; this pressure measurement, in conjunction with the duty cycle administered to the solenoid valve via a pulse-width modulation (PWM) control mechanism, dictated the rate of ink discharge at the nozzle aperture. Optimal parameters for achieving layer uniformity and thickness were established at an ink reservoir pressure ranging approximately from 0.4 to 0.6 bar. In this investigation, direct-acting micro-solenoid valves were implemented, which function in a binary state, either fully open or fully closed. To modulate the valves, a meticulously designed Pulse Width Modulation (PWM) control system was instituted, segmenting the voltage into a sequence of "on" and "off" pulses while varying the duty cycle. By manipulating the amplitude or temporal duration of the voltage pulses, the opening duration of the valve was regulated, thereby enabling the control of the flow rate. In this study, a duty cycle of 50% at a frequency of 200 Hz

was utilized. The PWM signal was generated utilizing an ARDUINO UNO board and was managed through a LabVIEW programming interface. The velocity of the substrate was maintained at a constant rate of 10 mm/sec. The digital representation was generated employing Microsoft® 3D Builder software, utilizing a parallelepiped configuration with dimensions of 50 × 25 × 0.5 mm for the deposition of the suspension. The digital representation was subsequently processed utilizing the open-source software Slic3r, which is widely adopted for the generation of GCode files pertinent to 3D printing applications. Experimental assessments were executed at a controlled ambient temperature of 25 °C, culminating in the formation of a solid film printed onto textured fabrics, with a standoff distance established at 1250 µm.

## 2.3 Characterization

### 2.3.1 Coatings characterization

The structural characteristics of the films were investigated using an FT-IR Nicolet iS20 (Thermo Scientific) within the range of 600–4000 $cm^{-1}$ to identify the presence of functional groups present on the sample surface. Thermal analysis of the coatings, both before and after the curing process, was performed using a DSC instrument (Q100; T.A. Instruments, USA). The samples were placed in aluminum pans and heated at a rate of 10 °C/min, spanning a temperature range from −20 °C to 230 °C. For FTIR and DSC analysis, the coating solutions were directly cast onto silicone mold, with solvent evaporation followed by UV light curing. The cured hybrid coating materials were then detached from the silicon substrates for further characterization.

### 2.3.2 Solution characterization for digital deposition

The critical parameters for achieving optimal printing performance in inkjet printing, as mentioned above, include the solution's viscosity, density and surface tension. Then, to evaluate these parameters, viscosity, surface tension, density and pH were measured for the sol–gel solutions prehydrolized for 1 h. The density of solutions was determined by weighing 1 mL of the solution three times using an analytical balance. Viscosity measurements were carried out using a rheometer (RheoStress RS100, HAAKETM) with a cone-plate tool (60 mm diameter, 1° angle). Surface tension was analyzed using a manual tensiometer K6 (KRÜSS GmbH)

### 2.3.3 Textile fabrics characterization

To evaluate the effect of coatings on the final properties of textile fabrics, scanning electron microscopy (SEM) images were collected using thermoionic emission microscope (Hitachi S-2300A, dedicated software: Thermo Noran NSS) operating at a working bias of 5 kV and 10 kV. These images were used to evaluate the surface topography. For high-resolution imaging, all samples were sputter-coated with an Au-Pd alloy prior to SEM observation. The impact of the coatings on fabric color was assessed by performing color measurements on both uncoated and coated samples using the CIELAB method, which provided L*, a*, and b* values. The color change, ΔE*, between the uncoated and coated surfaces was calculated, where ΔL* represent the change in lightness, Δa* the change in the red-green axis, and Δb* the change in the yellow-blue axis.

To evaluate the wetting properties of the textile substrates after functionalization with chitosan- based coatings, contact angle measurements were performed by using OCA 20 apparatus from DataPhysics Instruments GmbH, Filderstadt, Germany. Static contact angles were measured with distilled water droplets of 5 µl volume, and the contact angle measurements were performed 30 s after the droplet deposition. The results were calculated by averaging 10 measurements taken from different area of the surfaces. The stability of the coatings was assessed by following hydrolytic degradation in hot water (~60 °C), involving multiple washing cycles. Then, after each 30-min hot water cycle, contact angle measurements and weight change were conducted.

To evaluate the easy-cleaning efficiency of the modified cotton textiles, liquid contaminants such as a 0.01% Methylene blue (MB) solution were used [42]. Methylene blue, a cationic dye widely employed in numerous industries like textiles, is commonly used for dyeing cotton, silk, and wool fabrics [43]. In this study the contact angle measurements were performed by using droplets of 10 µl volume.

The friction coefficient was determined at room temperature using a ball-on-disk instrument (POD 4.0, Ducom Instruments Pvt. Ltd., India). A stainless-steel ball (316-L) with a diameter of 10 mm was used, applying anormal force of 2 N. The test duration was set at 600 covering a total distance of 6.28 m. For each specimen, three replicate tests were carried out and the average friction coefficient (COF) was reported. The COF was measured using a load cell to monitor the tangential force on the pin-holding support. Contact angle measurements were also performed after the abrasion tests.

Surface roughness was evaluated using a stylus profilometer with a 2 µm radius tip (Hommel tester W55, Jenoptik Industrial Metrology GmbH, Germany) and applying a 1 mN contact force. The selected cut-off lengths were 0.25 mm and 2.5 mm. Then, roughness parameters measured included the average surface roughness (Ra) root-mean-square roughness (Rq) and the maximum height of profile (Rz)

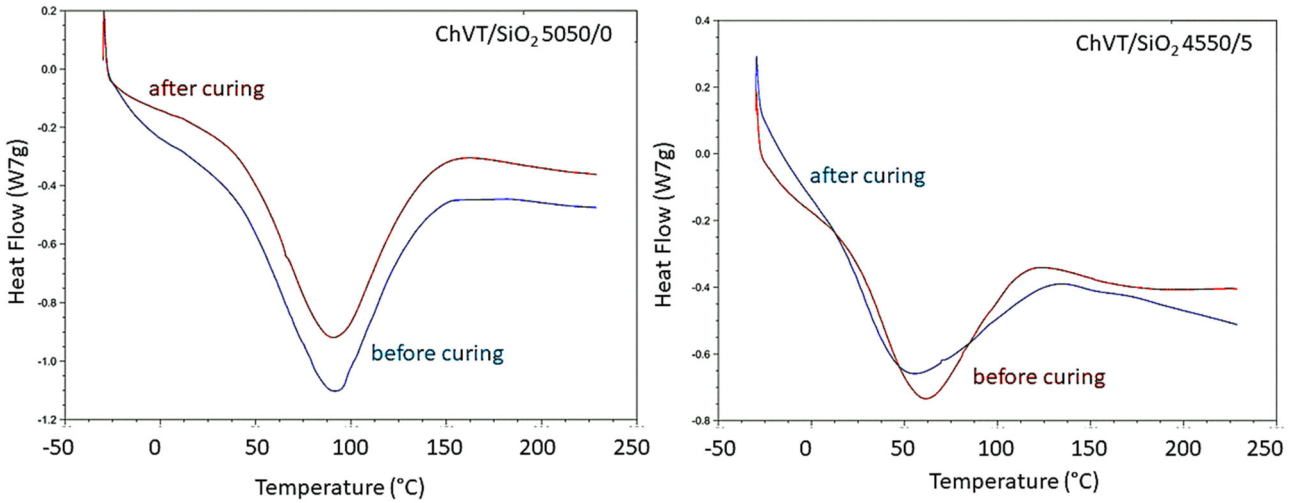


**Fig. 2** Comparison of heating curves before and after UV curing

## 3 Results

### 3.1 Coatings and textile fabrics characterization

Differential scanning calorimetry was used to characterize the chitosan-based films before and after UV curing process. As shown in Fig. 2, an endothermic peak due to the presence of residual solvent and byproducts in the coatings composition is observed before and after curing. Furthermore, the DSC curve in Fig. 3 highlights the necessity of a post-curing step at approximately 80 °C to effectively remove these residual solvents and byproducts from the sol–gel process. The rapid curing process associated with UV technology likely hinders the complete evaporation of these volatiles, emphasizing the importance of additional thermal post-treatment.

Figure 4 shows the FTIR results of ChVT/$SiO_2$ 5050/0 sample before and after curing process. The data clearly highlight that the absorption peak related to ethylene group and Si-O-C of VTMS decrease after UV curing, indicating a combined polymerization of VTMS and chitosan. The main difference in the FTIR spectra of samples, before and after UV curing, is the increase in the band at 1300 $cm^{-1}$, characteristic of the -CH stretching peak and the decrease in the intensity of the band at 961 $cm^{-1}$ and 762 $cm^{-2}$. These bands correspond to the stretching vibrations of the amine group of chitosan and absorption peaks of ethylene groups. Moreover, the appearance of absorption peak at 800 $cm^{-1}$, related to symmetrical stretching vibration of Si-O, and the increase of CO peak at 1720 $cm^{-1}$ suggest a reaction between the functional groups of chitosan and organic silanes during the post curing process [44]. The peak at 1400 $cm^{-1}$ is attributed to the deformation mode of $CH_2$ vibrations present in the vinyl group [45] while the amide I group of chitosan at 1630 $cm^{-1}$ shifts to lower wavenumber of 1600 $cm^{-1}$. This is due to the hydrogen bonding between silanol-hydrogen and carbonyl group. Finally, the change observed in the peak at approximately 1100 $cm^{-1}$ indicates the formation of a more highly ordered Si-O-Si network [46].

Figure 5 shows the FTIR spectra of samples after the addition of TEOS, labeled as ChVT/$SiO_2$ 4550/5. An increase in the intensity of bands associated with OH species (3300–3500 $cm^{-1}$) is observed, particularly around 3400 $cm^{-1}$, indicates enhanced hydrogen bonding and electrostatic interactions in the TEOS-modified films [47, 48] Furthermore, after the curing process, the narrower peak in the 1050–1100 $cm^{-1}$ region suggests a higher degree of order within the Si-O-Si network [46]. The appearance of a new peak at 1550 $cm^{-1}$ can be associated to electrostatic interactions between the protonated amine group ($–NH_3^+$) of chitosan and $O^-$ (hydroxyl) group of TEOS following the hydrolysis and condensation reaction. Microscopic images of the coated textiles in Fig. 6 confirm that the 2 wt.% sol–gel solution does not form a continuous coating over the fabric but instead covers individual fibers without bonding them together. The larger spaces between whole yarns remain unaffected, thus preserving the textile's original properties. At higher solution concentrations, a thin film layer forms between individual fibers, as shown in the higher-magnification images in Fig. 7. In all cases, no aggregates are visible, indicating a homogeneous distribution of the coating on the fibers. Furthermore, the absence of gaps between the film and the fibers, suggests good/strong adhesion between them.

Given the importance of preserving fabric properties, the initial screening of films focused on the coating's on fabric color. In fact, after deposition and drying, a noticeable color variation was observed on treated samples with respect to untreated fabrics. These differences were measured through

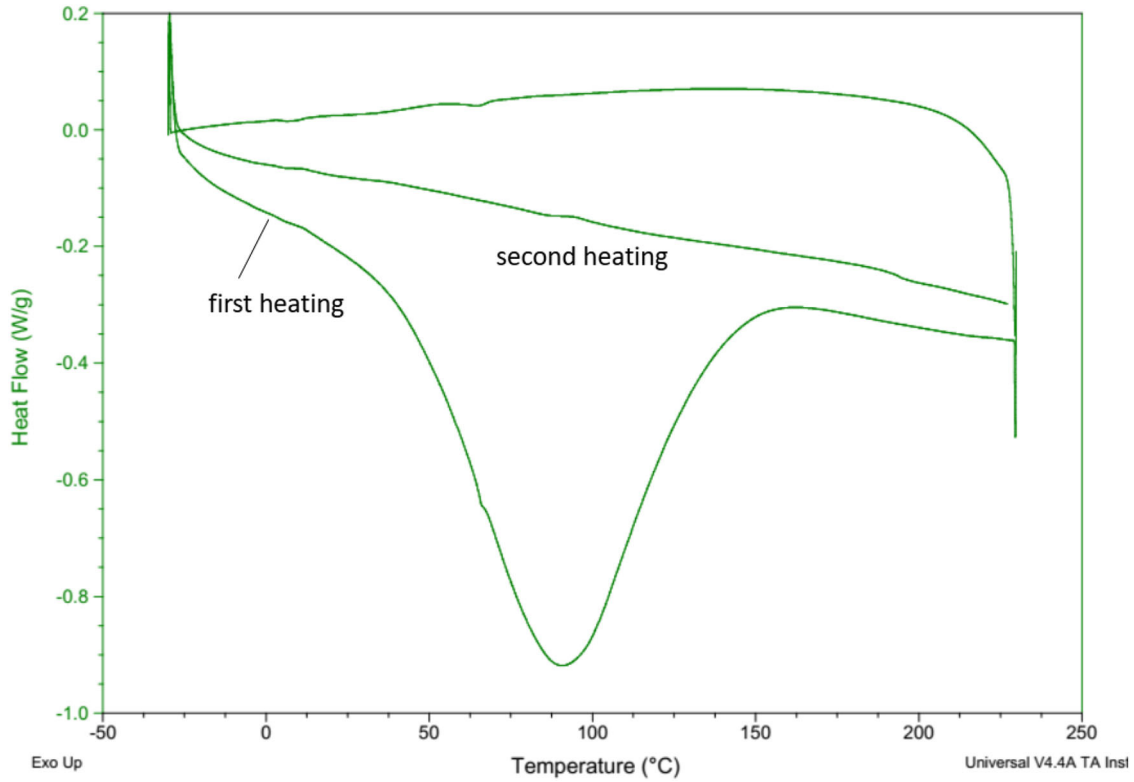


**Fig. 3** Heating and cooling curves obtained from DSC of the sample ChVT/$SiO_2$ 5050/0

instrumental analysis of color variation, as shown in Table 2.

The color change of substrates was significant after the application of solution at higher concentration (5 wt. %). In particular, in all samples exhibited a substantial increase in b* values, indicative of chitosan's yellow grade. This behavior was particularly pronounced for the coatings obtained at higher concentration and applied on polyester fabrics. However, the measured color variations, ΔE*, were moderate and acceptable (between 2.40 and 3.50) for lower solution concentration.

Table 3 presents the results regarding the hydrophobic properties of textile fabrics, as determined by contact angle measurements. The application of chitosan-based coatings significantly increased wettability angles from 0° to about 110–120° (Fig. 8). Polyester fabrics exhibited higher hydrophobicity after treatment with solution at different concentrations. Conversely, cotton fabrics, demonstrated higher contact angles at lower concentrations. Specifically, the water contact angle increased gradually when a 2 wt% solution was applied to both the fabrics. Importantly, no hydrophobic properties were observed with coatings composed solely of chitosan.

Based on the roughness values reported in Table 4, we can suppose that variations in hydrophobicity are partially influenced by differences in surface roughness and, consequently, by the different textures of the fabrics. The average roughness values of PE fabrics are approximately 2-3 times greater than those of cotton fabrics [49].

Hydrolytic degradation was assessed through hot water immersion and multiple washing cycles to evaluated the stability of the coatings. By plotting the change in weight of coated samples against treatment time (Fig. 9), a slight weight decrease after the first washing cycle may be attributed to the removal of residual solvents or by-products. As shown in Table 5, the hydrophobic properties improved after washing. This is likely due to the removal of residual solvent and unreacted hydroxyl groups, particularly in the case of cotton fabrics. To confirm these findings, washing cycle tests were replicated under the same conditions for samples coated with a 2 wt.% solution. Contact angle values were evaluated after 30 min of washing. The results in Fig. 10 confirm that high-temperature washing cycles effectively remove residual by-products from hydrolysis and condensation reactions during sol–gel processing, especially from the cotton substrate, leading to enhanced final hydrophobic properties.

The stain resistance test aimed to evaluate the resistance of the textile fabrics to the action of staining agents without the alteration of color. Table 3 presents the contact angle values of methylene blue (MB) droplets on both uncoated and coated textile fabrics. As confirmed by the optical

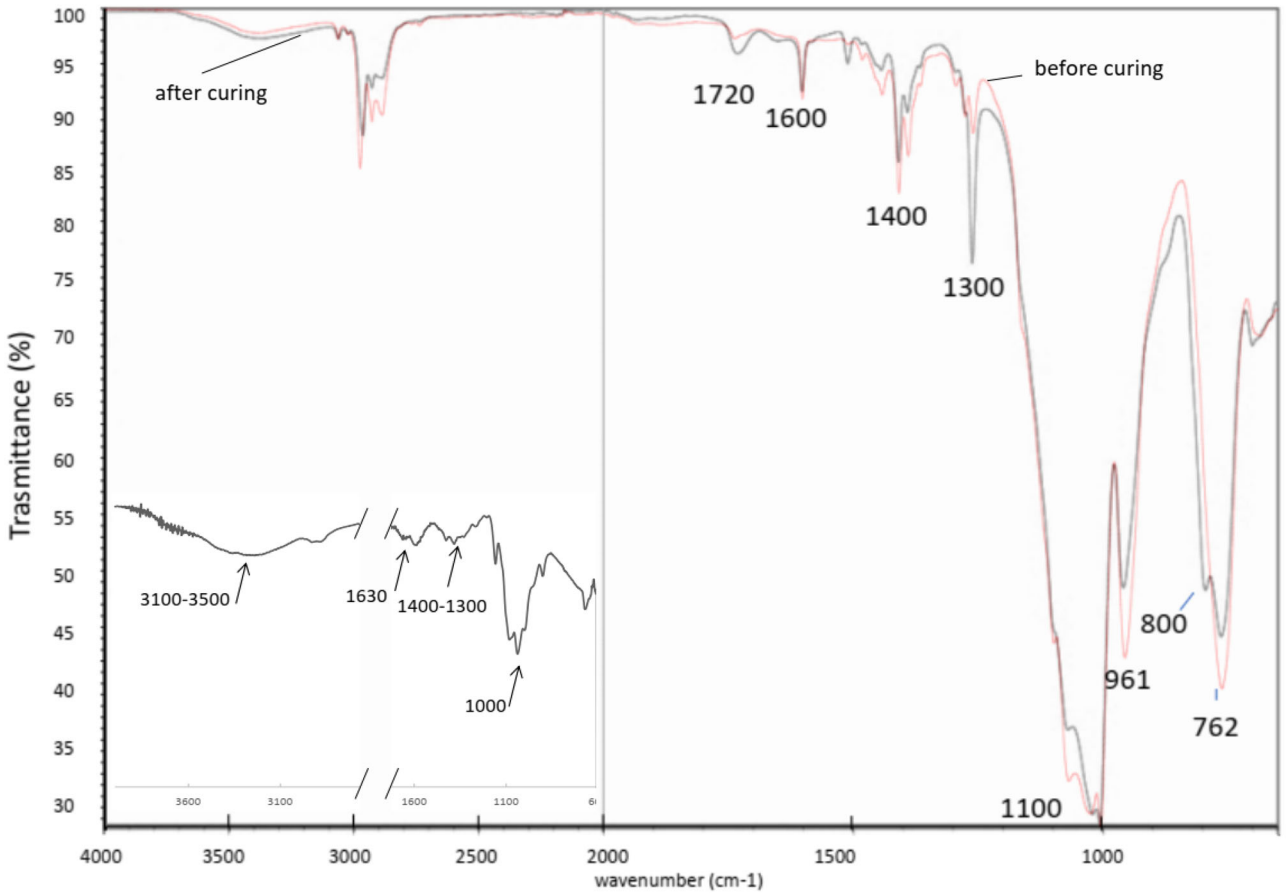


**Fig. 4** FTIR spectra of sample ChVT/$SiO_2$ 5050/0 before and after curing process and FTIR spectrum of chitosan

images in Fig. 11, untreated control fabrics exhibited a contact angle of 0°, indicating complete absorption of the dye.

The application of chitosan-based coatings imparted a degree of stain resistance, increasing MB contact angles to approximately 120–130°. This effect was particularly noticeable in polyester fabrics. On uncoated polyester, MB droplets were rapidly absorbed, whereas on coated samples, they remained on the surface with a high contact angle. Moreover, with a slight tilt of the surface, the droplets rolled off easily, demonstrating significant stain resistance (see Fig. 12a). In contrast, no stain resistance was observed for either uncoated and coated cotton fabrics. As showed in Fig. 12b, the droplets remained pinned to the surface even after tilting the substate by 180°. These contrasting results suggest that differences in fabric texture may involve different physical or chemical interactions. Capillary action might occur between cotton fabrics and methylene blu dye or variations in the density of functional groups on the surface is a crucial parameter in controlling MB dye adsorption mechanisms.

The practical applications of a hydrophobic coating are significantly influenced by its resistance to mechanical abrasion, which can compromise its water repellency and integrity.

To assess this, the abrasion resistance of both neat textile fabrics and coated samples was investigated by tribological test to simulate the abrasion that occurs during cleaning operations. Evaluating the abrasion resistance of textile is very complex due to the influence of various factors such as structure of the yearns, mechanical properties of the fibers, condition of the tests etc. In this work, tribological tests were conducted to obtain an indication of the relative friction coefficient (COF). In fact, by reducing the COF values, energy losses due to friction, wear or heat generation can be minimized. To evaluate the effect of chitosan-based films on the improvement of abrasion resistance of textile fabrics, the friction values were plotted as a function of number of sliding cycles (rotational cycles).

As showed in Fig. 13, the results are promising, with lower COF values measured for the coated textile fabrics. The friction curves of coated samples present significantly different COF depending on the solution concentration and composition.

When using a solution with a lower concentration, no increase in wear resistance was observed. However, a

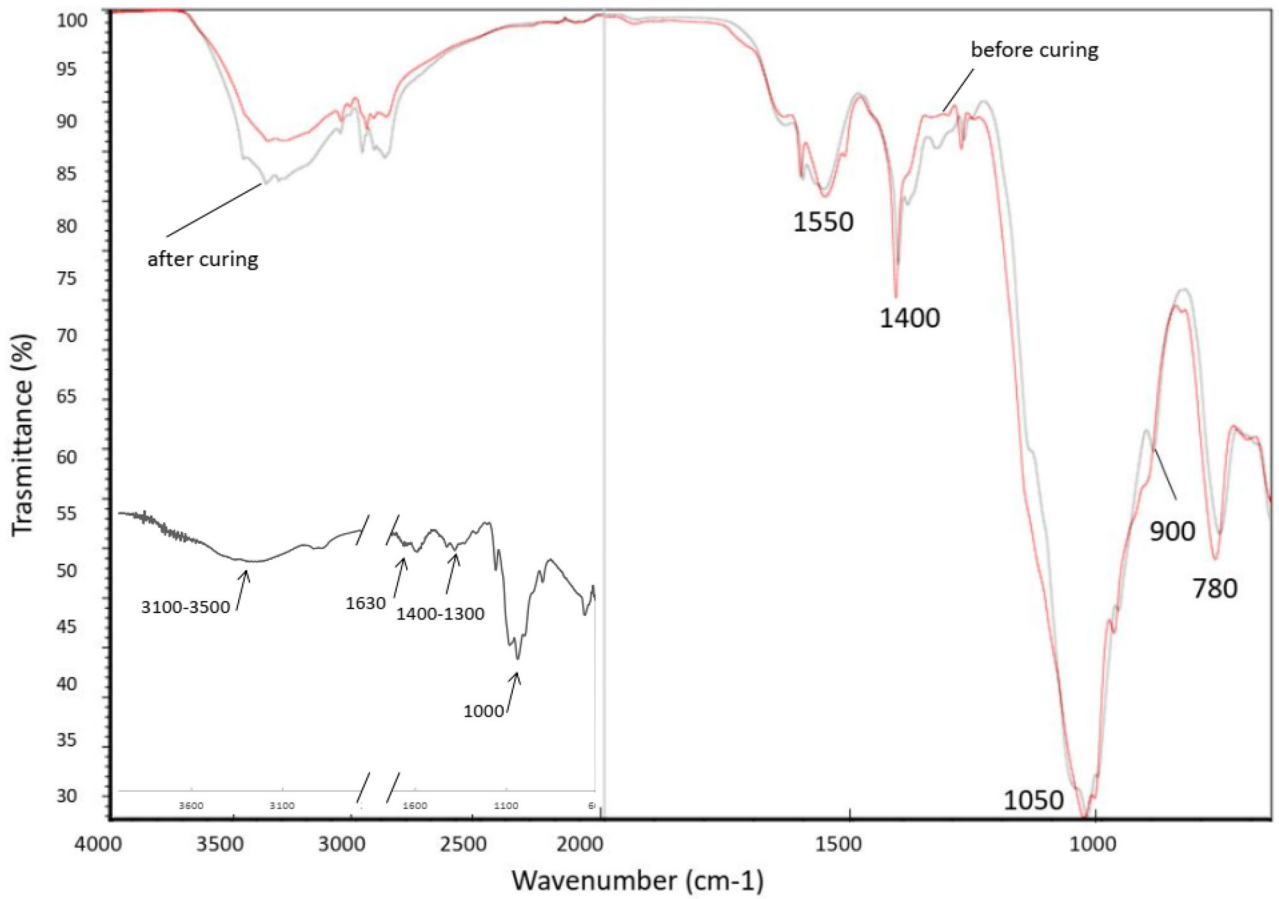


**Fig. 5** FTIR spectra of sample ChVT/$SiO_2$ 4550/5 before and after curing process and FTIR spectrum of chitosan

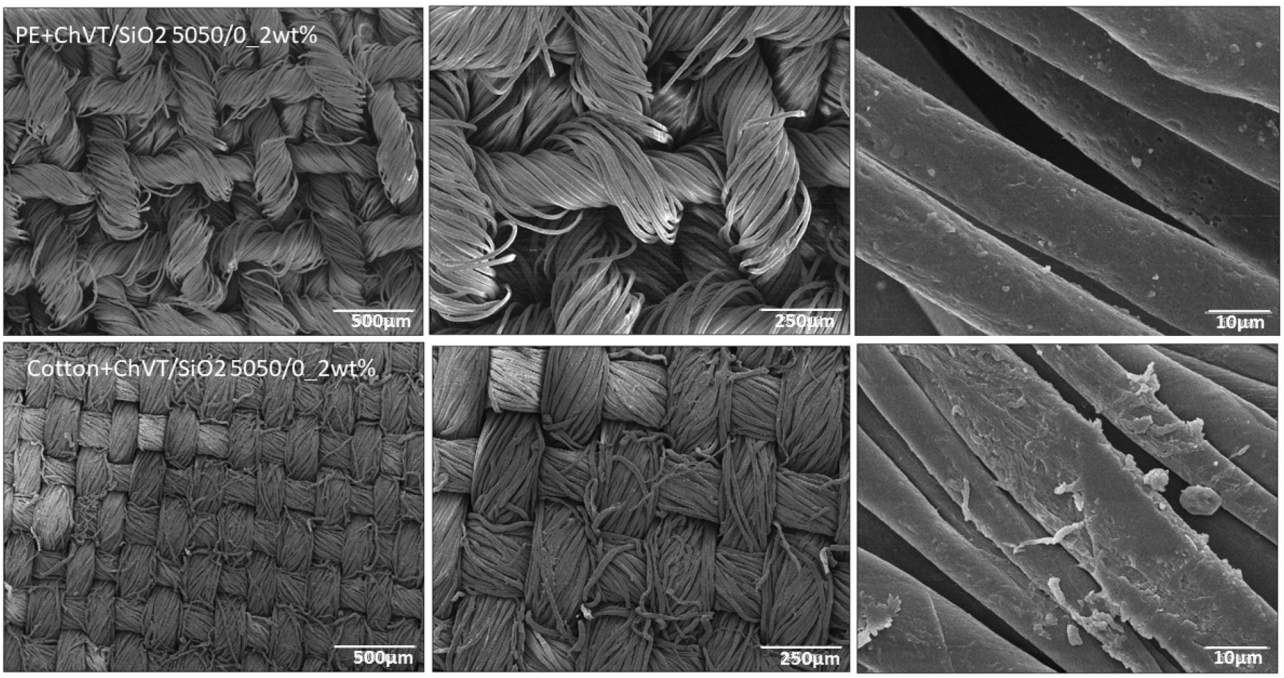


**Fig. 6** SEM images at 50×, 100× and 2000× of polyester and cotton fabrics after application of solgel solution at 2 wt.% of concentration

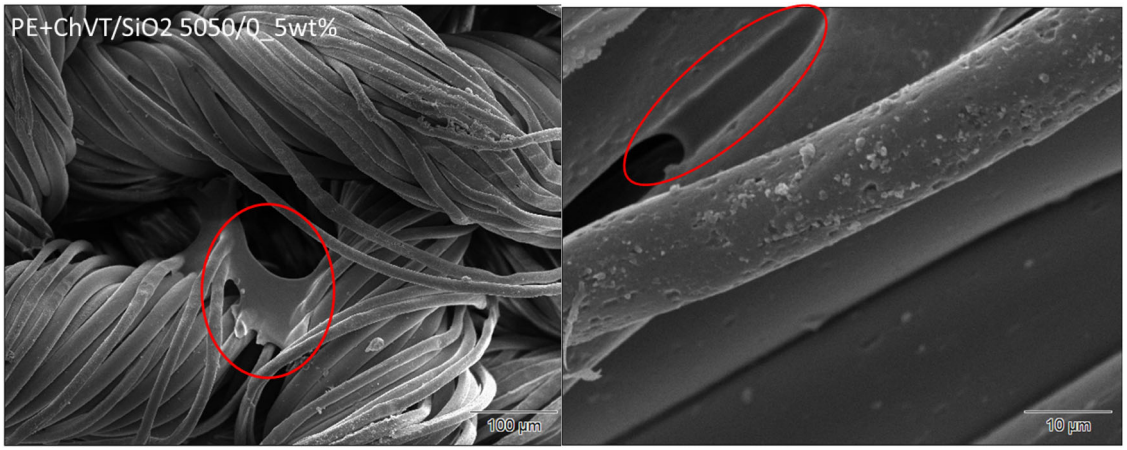


**Fig. 7** SEM images at 200× and 2000× of polyester fabrics after application of solgel solution at 5 wt.% of concentration

**Table 2** Average value and standard deviation of color parameters and color change, (ΔE*), due to the treatments on polyester and Cotton fabrics

| Sample ID | L* | a* | b* | ΔE* |
|---|---|---|---|---|
| Polyester fabric | 93.45 | −0.43 | 1.09 | — |
| PE+Ch/$SiO_2$ 100/0_5wt% | 91.05 | −0.58 | 6.02 | 5.60 |
| PE+ChVT/$SiO_2$ 5050/0_5wt% | 91.04 | −0.55 | 5.93 | 5.40 |
| PE+ChVT/$SiO_2$ 4550/5_5wt% | 90.59 | −0.64 | 7.21 | 6.75 |
| PE+ChVT/$SiO_2$ 5050/0_2wt% | 92.35 | −0.59 | 4.14 | 3.24 |
| PE+ChVT/$SiO_2$ 4550/5_2wt% | 92.9 | −0.63 | 3.47 | 2.44 |
| Cotton fabric | 93.44 | −0.44 | 1.08 | — |
| Cot+Ch/$SO_2$ 100/0_5wt% | 92.45 | −0.28 | 3.55 | 2.83 |
| Cot+ChVT/$SiO_2$ 5050/0_5wt% | 92.33 | −0.25 | 3.43 | 2.61 |
| Cot+ChVT/$SiO_2$ 4550/5_5wt% | 92.5 | −0.35 | 3.67 | 2.76 |
| Cot+ChVT/$SiO_2$ 5050/0_2wt% | 93.4 | −0.04 | 0.39 | 0.80 |
| Cot+ChVT/$SiO_2$ 4550/5_2wt% | 93.58 | −0.01 | 0.23 | 0.96 |

L*, a*, b*, etc are the coordinates defined by the Commission Internationale de l'Eclairage (CIE) (CIELAB method)

**Table 3** Average value and standard deviation of static contact angles with water($\theta_{H2O}$) and with methylene blu ($\theta_{MB}$) for the tested samples

| Sample ID | $\theta_{H2O}$ | $\theta_{MB}$ |
|---|---|---|
| Polyester fabric | 0 | 0 |
| PE+Ch/$SiO_2$ 100/0_5wt% | 0 | 0 |
| PE+ChVT/$SiO_2$ 5050/0_5wt% | 130 ± 4 | 123 ± 6 |
| PE+ChVT/$SiO_2$ 4550/5_5wt% | 120 ± 3 | 122 ± 6 |
| PE+ChVT/$SiO_2$ 5050/0_2wt% | 127 ± 3 | 128 ± 6 |
| PE+ChVT/$SiO_2$ 4550/5_2wt% | 132 ± 2 | 126 ± 4 |
| Cotton fabric | 0 | 0 |
| Cot+Ch/$SO_2$ 100/0_5wt% | 10 ± 3 | 0 |
| Cot+ChVT/$SiO_2$ 5050/0_5wt% | 105 ± 4 | 94 ± 3 |
| Cot+ChVT/$SiO_2$ 4550/5_5wt% | 109 ± 3 | 115 ± 5 |
| Cot+ChVT/$SiO_2$ 5050/0_2wt% | 113 ± 5 | 113 ± 6 |
| Cot+ChVT/$SiO_2$ 4550/5_2wt% | 117 ± 2 | 110 ± 11 |

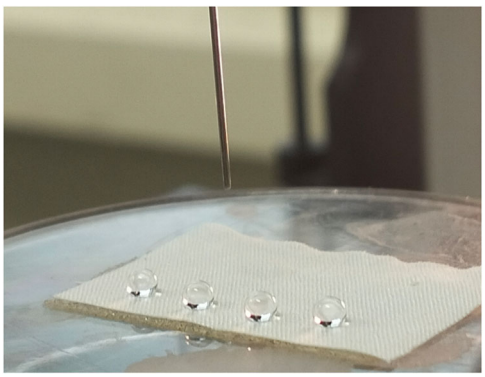

**Fig. 8** Image of water drops on the surface of modified PE fabrics

significant decrease in the coefficient of friction (COF) was noted for cotton fabrics modified with the chitosan-based solution without silica from TEOS and at a higher concentration. This reduction in COF is likely attributable to the increased thickness of the coating.

To assess the effect of abrasion on hydrophobic properties, water contact angles were measured post-testing (Table 6). A minor reduction (~10°) in contact angle was observed, indicating that chitosan-based coatings maintained sufficient adhesion and durability. This result aligns with findings from our previous work [50], which demonstrated the intrinsic lubricity of chitosan-silica sol–gel coatings

## 3.2 Textile fabrics characterization after digital deposition

Based on the results from the first part of the study, we decided to use the lowest concentration solution for digital deposition. As highlighted in a previous work [19], the solution's chemical and physical properties are crucial parameters for achieving homogeneous deposition during digital printing. Specifically, viscosity, density, and surface tension

must fall within an appropriate range to ensure compatibility with the printing process, as detailed in the experimental section. Table 7 presents the final properties of the sol–gel solution for our system. Notably, to increase viscosity from its initial 6–7 mPa*s, the sol–gel solution underwent an extended reaction time of 1 h before application onto the substrates.

As evident in Table 7, extending the reaction time of the sol–gel solution to 1 h resulted in a significant viscosity increase, making the solution more suitable for digital deposition by preventing splatter and the formation of undesirable satellite droplet formation. Furthermore, a comparison of the viscosity results indicates that the presence of silica derived from TEOS can enhance the viscosity of the solution, while the surface tension values remain similar for both compositions.

Digital deposition enabled the achievement of a highly homogeneous coating distribution on the fibers, as shown in Figs. 14 and 15. The absence of aggregates and gaps between the fibers and the coating indicates excellent adhesion and compatibility of the chitosan-based solution and the textile fabrics.

Table 8 presents the contact angles values for the hydrophobized fabrics, indicating good hydrophobizing ability for both solution compositions on both textile substrates. Note that the contact angles on cotton substrates exceeded the 120°, suggesting a more homogenous coating with a more regular submicrostrucure. This is supported by higher magnification SEM images in Figs. 15 and 16, which reveal a more uniform morphology compared to that observed in Fig. 7.

## 4 Discussion

This research explores the potential of chitosan-based hybrid coatings, developed through a combination of sol–gel processes and UV irradiation, for enhancing textile fabrics. These coatings aim to provide desirable properties like hydrophobicity, stain resistance, and durability against washing. By integrating chitosan, an environmentally friendly alternative to harmful chemicals, this approach addresses the pressing ecological concerns associated with the textile industry, a sector widely recognized for its significant environmental footprint [51, 52].

Moreover, liquid-repellent textile fabrics find ubiquitous use in both consumer products and technical applications [51]. In the final part of this work, a 3D inkjet printing process was proposed as an efficient method for creating homogeneous films with hydrophobic properties, offering significant advantages. Specifically, the 3D inkjet printing process involving layer-by-layer deposition, similar to other 3D printing techniques, provides high precision in dispensing solution volumes localizing the solution on the surface during the injection process. This ensures more efficient deposition of the precursor solution while reducing material consumption. Moreover, digital inkjet printing has the potential to serve as a crucial clean technology for textile fabrics.

Unlike previous studies, our research introduces a novel approach to developing hybrid sol–gel coatings. Specifically, we utilized a combination of chitosan and VTMS as a finishing agent combined with UV curing. Comparisons with existing studies show that the same level of hydrophobicity achieved using fluorinated silanes [8] or nanoparticles [8, 16, 17, 21] can be attained through the

**Table 4** Roughness parameters (Rq, Rz, Rt) of cotton and synthetic fabrics (PE)

| Sample | Rq (μm) | Rz (μm) | Rt (μm) |
|---|---|---|---|
| PE fabric | 16.3 ± 0.1 | 93 ± 17 | 143 ± 78 |
| Cotton fabric | 7.6 ± 0.5 | 31 ± 1 | 42 ± 7 |

**Table 5** Static water contact angles (θs) after several wash cycles in hot water for samples coated with the solution at 5 wt%

| Time of washing | PE + ChVT/$SiO_2$ 5050/0 *θs(deg)* | PE + ChVT/$SiO_2$ 4550/5 *θs(deg)* | Cot + ChVT/$SiO_2$ 5050/0 *θs(deg)* | Cot + ChVT/$SiO_2$ 4550/5 *θs(deg)* |
|---|---|---|---|---|
| 0 min | 127 ± 2 | 132 ± 3 | 105 ± 4 | 109 ± 3 |
| 30 min | 128 ± 1 | 134 ± 3 | 115 ± 3 | 129 ± 4 |
| 60 min | 134 ± 5 | 125 ± 7 | 119 ± 3 | 127 ± 2 |
| 90 min | 130 ± 1 | 132 ± 1 | 117 ± 2 | 121 ± 2 |

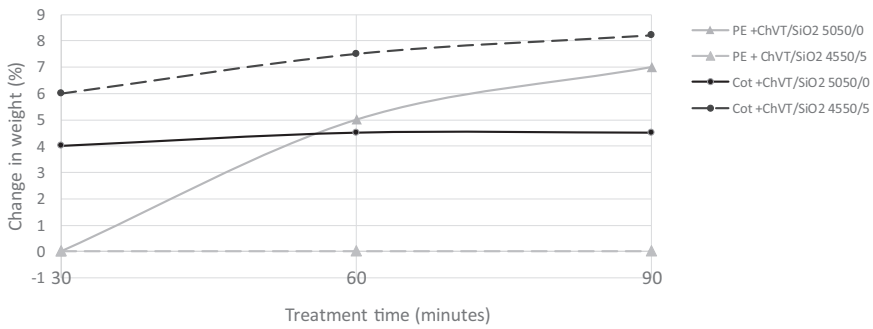


**Fig. 9** Change in weight (%) versus time for several wash cycles in hot water

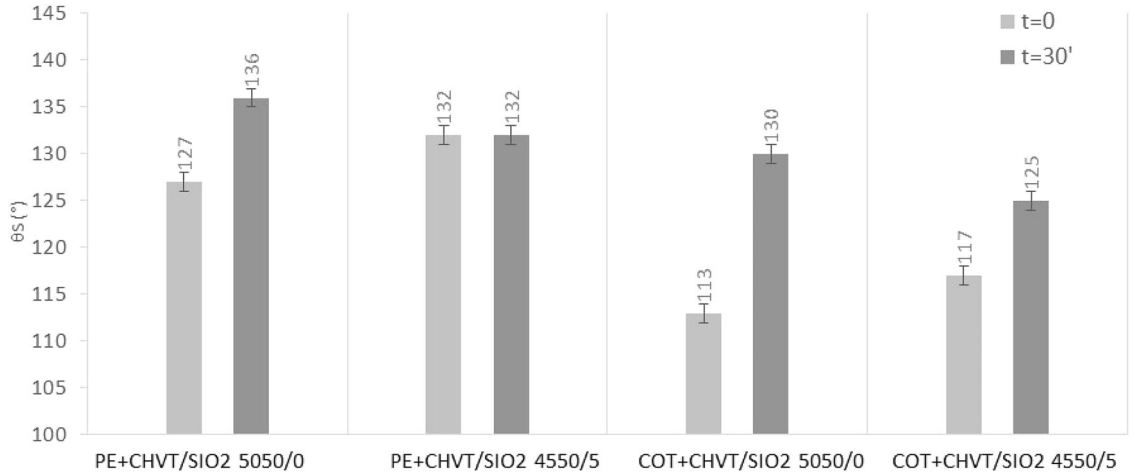


**Fig. 10** Static water contact angles (θs) of samples coated with the solution at 2 wt% of concentration and after 30 min of wash cycle in hot water

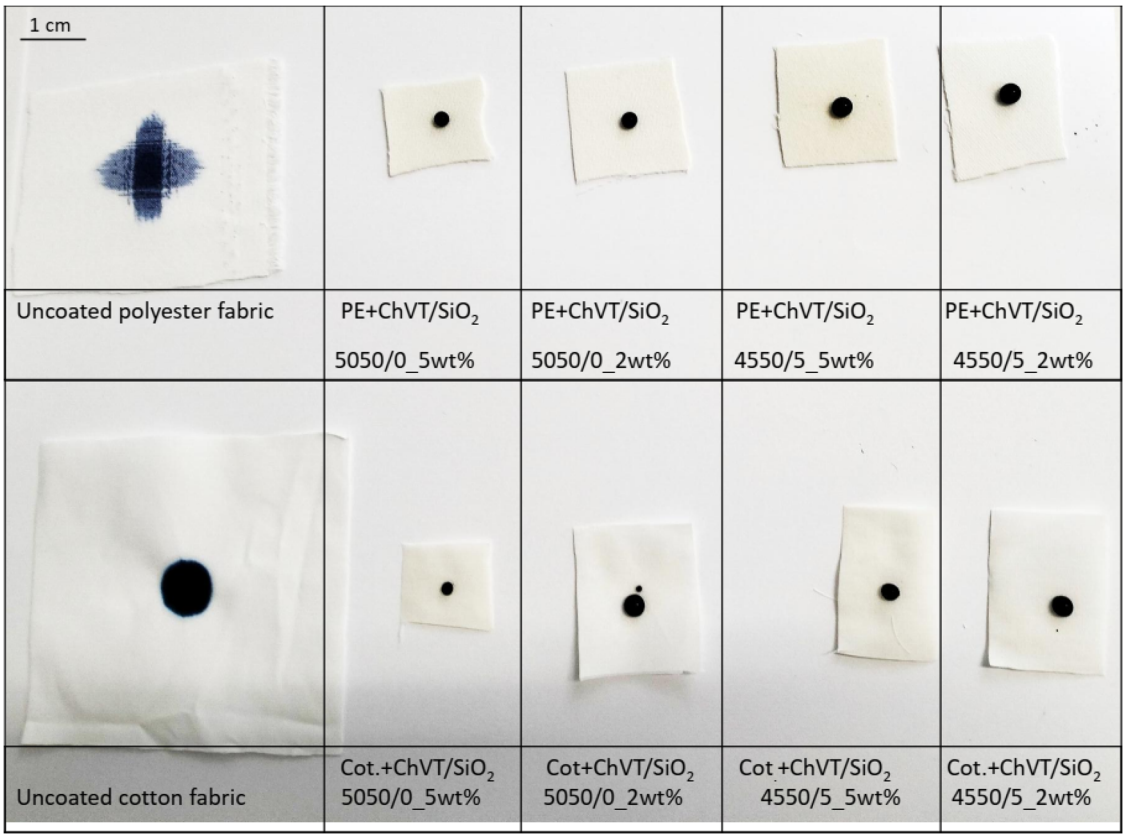


**Fig. 11** Optical mages of methylene blue (MB) stain placed on uncoated and coated textile fabrics

combination of a silane agent with chitosan, an environmentally sustainable raw material.

Moreover, the potential for depositing this type of solution onto textile fabrics using a 3D process, such as inkjet printing, has not been previously investigated.

The results obtained in the first part of this work indicate that the addition of VTMS is necessary to achieve hydrophobic properties. In fact, a solution based solely on chitosan does not alter the properties of textile fabrics, likely due to the hydrophilic nature of chitosan, as suggested by our findings and several studies [50, 53, 54].

To enhance hydrophobic properties, the chitosan-based sol–gel solution was modified with VTMS. This compound, containing silicon-oxygen bonds, can act as a finishing

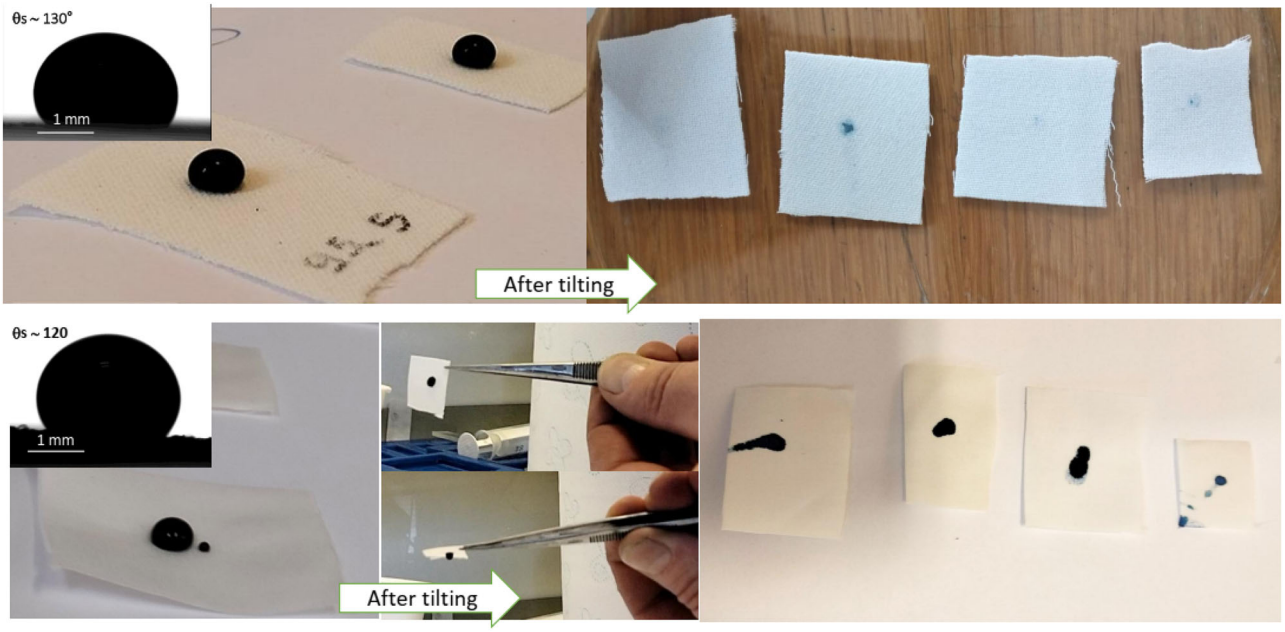


**Fig. 12** Optical images of methylene blue (MB) stain placed on (**a**) coated PE fabrics before and after substrate tilting and (**b**) on coated cotton fabrics before and after substrate tilting

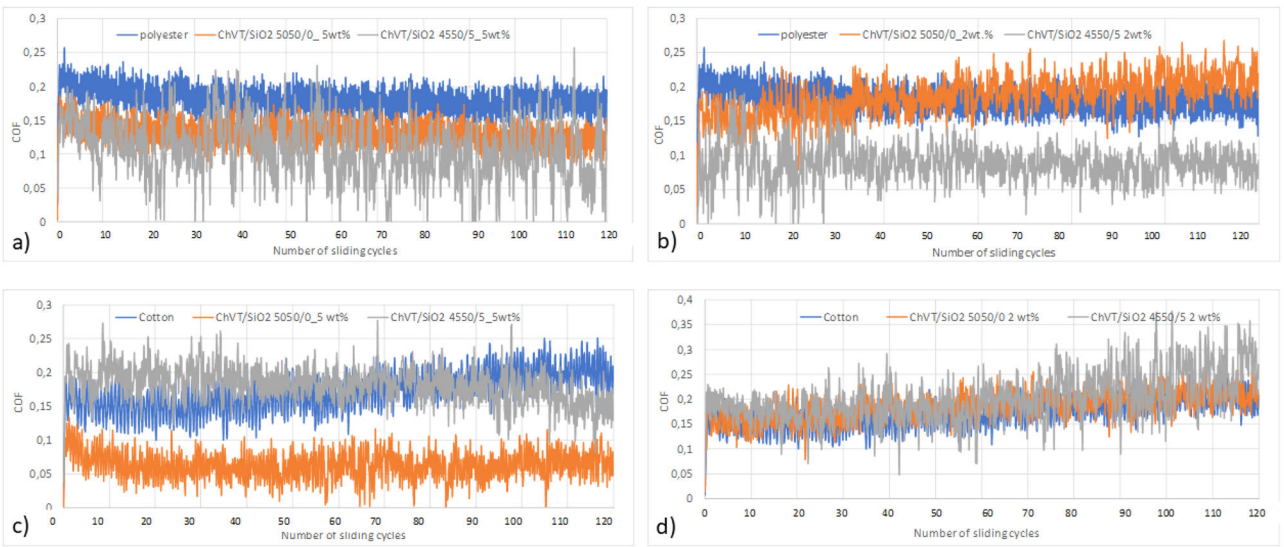


**Fig. 13** Friction coefficient measured during wear testing of **a** polyester substrate uncoated an coated with solution at 5 wt.% concentration, **b** polyester substrate uncoated an coated with solution at 2 wt.% concentration, **c** cotton substrate uncoated and coated with solution at 5 wt.% concentration and **d** cotton substrate uncoated and coated at 2 wt.% concentration

agent for textiles and, as reported in several studies [55, 56], facilitates the transformation of surface properties from hydrophilic to hydrophobic.

The addition of silica from TEOS enhances the hydrophobic properties by reducing electrostatic interactions between the coating and water. This effect is likely due to the increased interactions between chitosan and the M–OH groups of the silane compounds, as confirmed by the chemical analysis through FTIR. We can hypothesize that electrostatic interactions and the formation of covalent bonds between chitosan and the silane compounds occur, as shown in Fig. 16, which illustrates a schematic of the possible reactions between chitosan, VTMS, and TEOS after UV curing, hydrolysis, and condensation of the silica precursors.

The hydrophobic properties are maintained even after several cycles of hydrolytic degradation in hot water. The slight decrease in coating weight and the subsequent

increase in the contact angle after the first washing cycle were attributed to the removal of residual solvents or by-products from the hydrolysis and condensation reactions. Microstructural analysis and color change evaluation showed that a 2 wt.% solution results in more uniform coatings with stable hydrophobic properties and minimal color variations compared to untreated textile fabrics. Lower solution concentrations help preserve the original fabric color while maintaining hydrophobicity. As shown in Fig. 12, water-based methylene blue (MB) droplets maintain a spherical shape on the PE fabric surface, demonstrating the antifouling and self-cleaning properties associated with the surface hydrophobicity [57, 58].

However, cotton fabrics exhibited lower stain resistance, likely due to the high presence of hydroxyl groups on the fiber surface, which facilitates stain adhesion [59].

Building on the findings from this work, we explored the implementation of the sol–gel technique in combination with 3D inkjet printing technology to create films with a more uniform structure. The lower concentration solution was selected for this purpose. We optimized its chemical and physical properties, including viscosity, surface tension, and density, to achieve suitability for micro-solenoid inkjet 3D printing. As preformed in a previous work [19], to improve jettability and achieve a viscosity exceeding 10 mPa·s, the reaction time before application was increased from 30 min to 1 h. This approach is of interest because it can typically cover the viscosity range required for ejection of an inkjet droplet (normally around 1–30 mPa*s) [60].

The higher value of viscosity for ChVT/$SiO_2$ 4550/5 solution can be attributed to the grow and bonding of silica particles from hydrolysis and condensation reaction of TEOS.

Ideal droplet formation was observed for both solution compositions, indicating good printability. This was confirmed by SEM images, which revealed a highly uniform distribution of the film on the fiber surface. In particular, the homogeneous distribution of the film on cotton fibers increased the presence of hydrophobic side groups, inhibiting capillary action and thereby reducing water penetration. From the results obtained in the second part of this work, we can conclude that digital inkjet printing can serve as a crucial cleaner technology for textile fabrics. Furthermore, the presence of silica in the solution enhances printability without altering the final hydrophobic properties of the coatings.

Finally, although a known limitation of water-repellent coatings is their durability against abrasion and washing, our tests indicate that the coating retains its hydrophobicity even after multiple cycles in hot water. Measurements showed only a slight reduction in contact angle after abrasion, while no significant changes were observed after repeated washing, confirming the coating's robust hydrophobic nature.

These findings suggest how textile fabrics can be finished using chitosan-based sol–gel coatings in combination with UV curing process and 3D printing process as an environmentally friendly alternatives perfluorinated chemicals.

**Table 6** Average value and standard deviation of static water CAs ($\theta_S$) after abrasion test

| Sample ID | θs |
|---|---|
| PE+ChVT/$SiO_2$ 5050/0_5wt% | 129 ± 5 |
| PE+ChVT/$SiO_2$ 4550/5_5wt% | 115 ± 3 |
| PE+ChVT/$SiO_2$ 5050/0_2wt% | 120 ± 5 |
| PE+ChVT/$SiO_2$ 4550/5_2wt% | 117 ± 2 |
| Cot+ChVT/$SiO_2$ 5050/0_5wt% | 103 ± 4 |
| Cot+ChVT/$SiO_2$ 4550/5_5wt% | 108 ± 3 |
| Cot+ChVT/$SiO_2$ 5050/0_2wt% | 103 ± 5 |
| Cot+ChVT/$SiO_2$ 4550/5_2wt% | 108 ± 2 |

## 5 Conclusion

This research demonstrates the potential of chitosan-based hybrid coatings, developed through sol–gel processes and UV curing, as an environmentally friendly alternative to harmful and toxic agents. The study highlights the effectiveness of incorporating VTMS and TEOS into the chitosan-based solution to achieve durable hydrophobic properties. The addition of these silane compounds not only improves water repellency but also contributes to the stability of the coatings, as confirmed by the several chemical and physical characterization. Compared to untreated

**Table 7** Optimised physicochemical properties of sol–gel solutions for inkjet 3D printing process after 1 h of solgel process time

| | Solution Chitosan 2 wt.% | ChVT/SiO2 5050/0_2wt.% | ChVT/SiO2 4550/5_2w.t% | ChVT/SiO2 5050/0_2wt.% (after 1 h) | ChVT/SiO2 4550/5_2w.t% (after 1 h) |
|---|---|---|---|---|---|
| Surface tension (mN/m) | 52.13 ± 0.19 (27 °C) | – | – | 33.47 ± 0.35 | 35.17 ± 0.29 |
| Density (g/$cm^3$) | 0.95 | 0.90 | 0.88 | 0.90 | 0.88 |
| Viscosity (mPa*s) | 7–8 (27 °C) | 6–7 | 6–7 | 12–13 (27 °C) | 31–34 (27 °C) |
| pH | 3–4 | 3–4 | 3–4 | 3–4 | 3–4 |

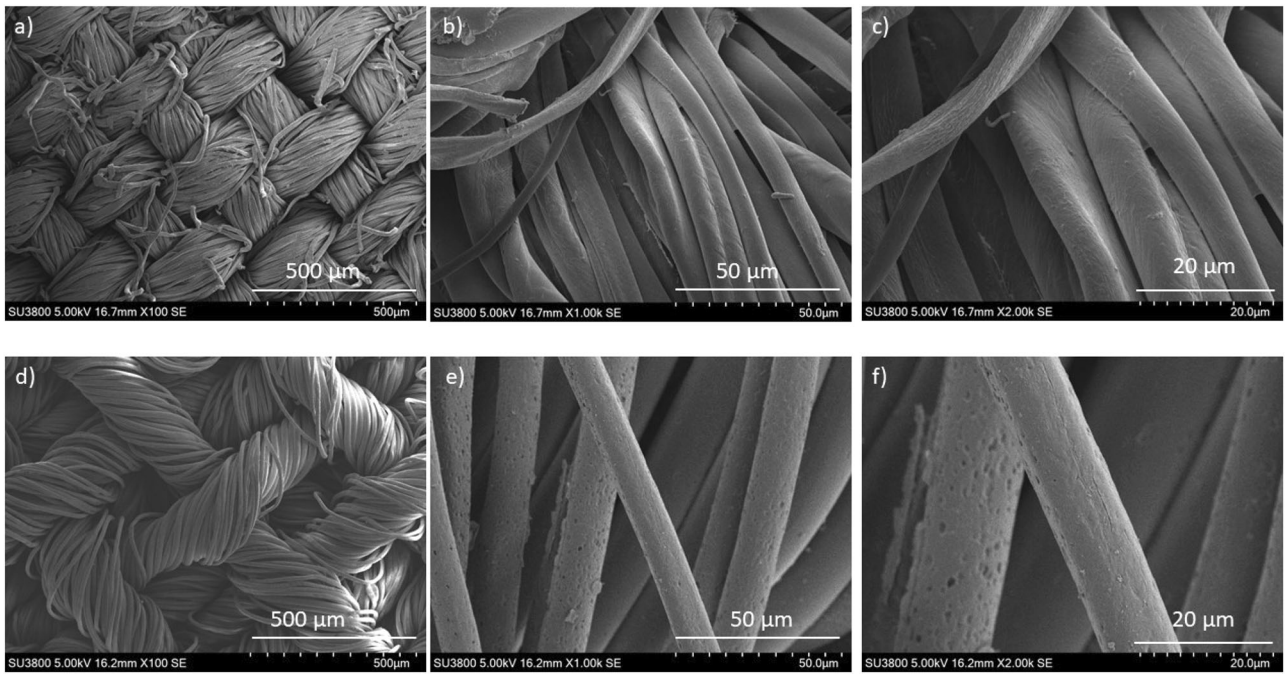


**Fig. 14** SEM images of Cot+ChVT/$SiO_2$ 5050/0 sample at 100× (**a**) 1000× (**b**) 2000× (**c**) and PE+ChVT/$SiO_2$ 5050/0 sample at 100× (**d**) 1000× (**e**) 2000× (**f**)

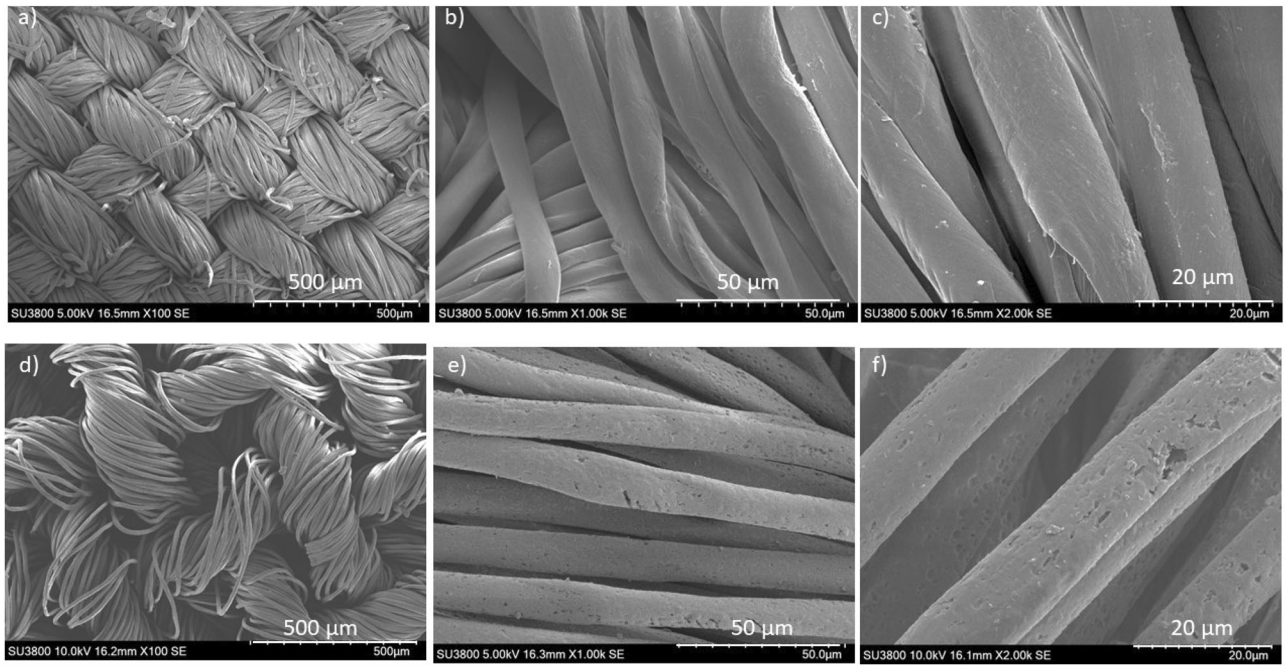


**Fig. 15** SEM images of Cot+ChVT/$SiO_2$ 4550/5 sample at 100x (**a**) 1000x (**b**) 2000x (**c**) and PE+ChVT/$SiO_2$ 4550/5 sample at 100× (**d**) 1000× (**e**) 2000× (**f**)

**Table 8** Static water contact angles (θs) of coated PE and cotton substrates using the inkject 3D printing process

| | PE+ChVT/$SiO_2$ 5050/0_2 wt.% | PE+ChVT/$SiO_2$ 4550/5_2 wt.% | Cot+ChVT/$SiO_2$ 5050/0_2 wt.% | Cot+ChVT/$SiO_2$ 4550/5_2 wt.% |
|---|---|---|---|---|
| $\theta s$ | 128 ± 1 | 134 ± 3 | 125 ± 3 | 129 ± 4 |

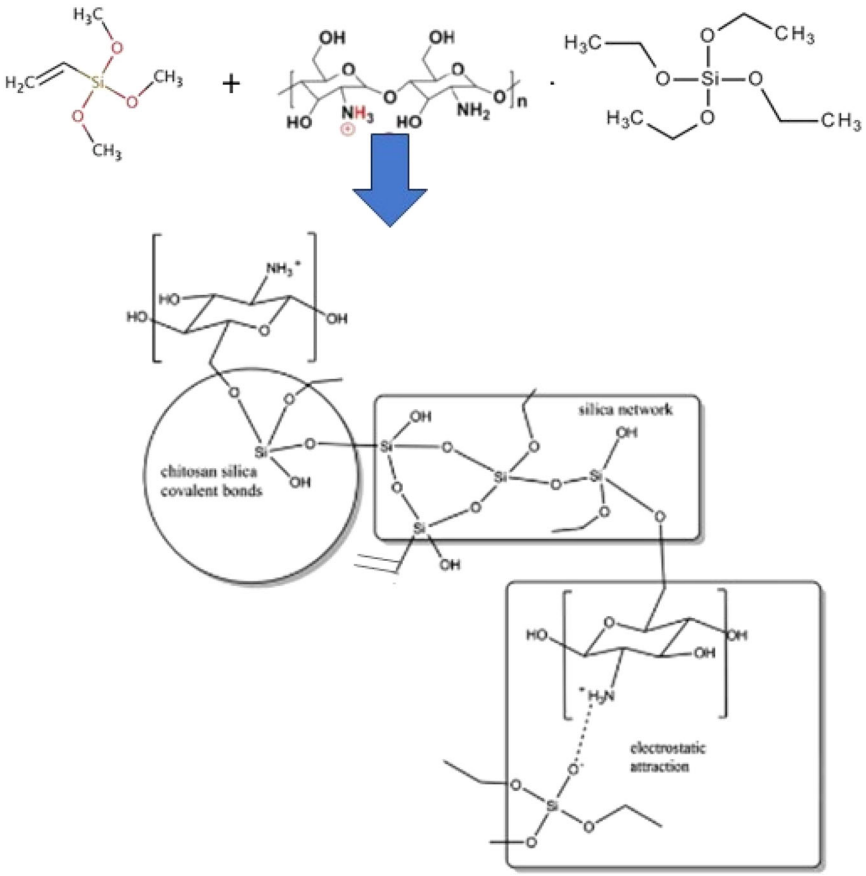


**Fig. 16** Schematic illustration of the possible reactions between chitosan, VTMS and TEOS

fabrics, the chitosan-based coatings demonstrated superior surface hydrophobicity that persisted even after multiple cycles of hydrolytic degradation in hot water and abrasion tests. Notably, applying the chitosan-based coatings at lower concentrations imparted multiple properties such as water repellence, stain resistance, and abrasion resistance while maintaining the substrate's color

Moreover, the use of digital inkjet printing as a deposition method proved to be an efficient and sustainable approach for fabric functionalization. By optimizing the chemical and physical properties of the sol–gel solution, we achieved precise control over coating distribution, ensuring uniform coverage with minimal material consumption. Additionally, the presence of silica in the solution facilitated printability without compromising the final properties of the coatings. These results indicate that chitosan-based sol–gel coatings could serve as a sustainable solution for outdoor apparel and functional textiles, combining water repellency, durability, and environmental compatibility. The integration of sol–gel technology with digital inkjet printing presents new opportunities for cleaner and more efficient textile processing methods, paving the way for future advancements in smart and functional.

These findings highlight the potential of sol–gel chitosan coatings as eco-friendly solutions for functionalizing both cotton and polyester, the two most widely used fibers in the textile industry. By utilizing renewable raw materials to modify textile surfaces instead of PFAS-based finishes, this approach aligns with sustainability principles and contributes to the transition toward a circular economy.

## Data availability

No datasets were generated or analysed during the current study.

**Acknowledgements** The authors acknowledge the technical support and facilities from the MatchLab (Material characterization Laboratory) of University of Florence and Santo Stefano S.p.A. (Prato) for the thermal and FTIR analysis.

**Author contributions** Rosa Taurino: Conceptualization, Data curation, Formal analysis, Investigation, Methodology, Writing – original draft, Review & editing. Maria Cannio: Validation, Formal analysis, Data curation, Writing – review & editing. Stefano Martinuzzi: Validation, Formal analysis, Data curation Stefano Caporali: Visualization, Validation, Formal analysis. Francesca Borgioli: Validation, Formal analysis, Visualization Emanuele Galvanetto: Visualization, Validation. Dino Boccaccini: Validation, Data curation, Formal analysis, Writing – review & editing.

**Funding** Open access funding provided by Università degli Studi di Firenze within the CRUI-CARE Agreement.

## Compliance with ethical standards

**Conflict of interest** The authors declare no competing interests.

**Publisher's note** Springer Nature remains neutral with regard to jurisdictional claims in published maps and institutional affiliations.



## References

1. Klinkhammer K, Hohenbild H, Hoque MT, Elze L, Teshay H, Mahltig B (2024) Functionalization of Technical Textiles with Chitosan. Textiles 4:70–90. https://doi.org/10.3390/textiles4010006
2. Ismail WNW (2016) Sol–gel technology for innovative fabric finishing-A review. J Sol Gel Sci Technol 78:698–707. doi: 10.1007/s10971-016-4027-y
3. Gashti MP, Pakdel E, Alimohammadi F (2016) Nanotechnology-based coating techniques for smart textiles. In Active Coatings for Smart Textiles. UK, Woodhead Publishing. 243–268
4. Mahltig B, Haufe H, Böttcher H (2005) Functionalisation of textiles by inorganic sol–gel coatings. J Mater Chem 15:4385–4398. https://doi.org/10.1039/B505177K
5. Bae GY, Min BG, Jeong YG, Lee SC, Jang JH, Koo GH (2009) Superhydrophobicity of cotton fabrics treated with silicananoparticles and water-repellent agent. J Colloid Interface Sci 337:170–175. https://doi.org/10.1016/j.jcis.2009.04.066
6. Hsieh CT, Wu FL, Yang SY (2008) Superhydrophobicity from composite nano/microstructures: Carbon fabrics coated with silica nanoparticles. Surf Coat Technol 202:6103–6108. https://doi.org/10.1016/j.surfcoat.2008.07.006
7. Yetisen A, Qu H, Manbachi A, Butt H, Dokmeci MR, Hinestroza JP, Skorobogatiy M, Khademhosseini A, Yun SH (2016) Nanotechnology in Textiles. ACS Nano 10:3042–3068. https://doi.org/10.1021/acsnano.5b08176
8. Gao Q, Zhu Q, Guo Y, Yang CQ (2009) Formation of Highly Hydrophobic Surfaces on Cotton and Polyester Fabrics Using Silica Sol Nanoparticles and Nonfluorinated. Ind Eng Chem Res 48:9797–9803. https://doi.org/10.1021/ie9005518
9. Böttcher H (2003) Modified Silica Sol Coatings for Water-Repellent Textiles. J Sol Gel Sci Technol 27:43–52. https://doi.org/10.1023/A:1022627926243
10. Textor T, Mahltig B (2010) A sol−gel based surface treatment for preparation of water repellent antistatic textiles. Appl Surf Sci 256:1668–1674. https://doi.org/10.1016/j.apsusc.2009.09.091
11. Daoud WA, Xin JH (2004) Low temperature sol-gel processed photocatalytic titania coating. J Sol Gel Sci Technol 29:25–29. https://doi.org/10.1023/B:JSST.0000016134.19752.b4
12. de Ferri L, Lorenzi A, Carcano E, Draghi L (2018) Silk fabrics modification by sol–gel method. Text Res J 88:99–107. https://doi.org/10.1177/0040517516676061
13. Mahltig B, Fiedler D, Simon P (2011) Silver-containing sol-gel coatings on textiles: Antimicrobial effect as a function of curing treatment. J Text Inst 102:739–745. https://doi.org/10.1080/00405000.2010.515730
14. Mahltig B, Fiedler D, Fischer A, Simon P (2010) Antimicrobial coatings on textiles-modification of sol-gel layers with organic and inorganic biocides. J Sol Gel Sci Technol 55:269–277. https://doi.org/10.1007/s10971-010-2245-2
15. Zahid M, Mazzon G, Athanassiou A, Bayer IS (2019) Environmentally benign non-wettable textile treatments: A review of recent state-of-the-art. Adv Colloid Interface Sci 270:216–250. https://doi.org/10.1016/j.cis.2019.06.001
16. Shen K, Yu M, Li Q, Sun W, Zhang X, Quan M, Liu Z, Shi S, Gong Y (2017) Synthesis of a fluorine-free polymeric water-repellent agent for creation of superhydrophobic fabrics. Appl Surf Sci 426:694–703. https://doi.org/10.1016/j.apsusc.2017.07.245
17. Yu M, Li P, Feng Y, Li Q, Sun W, Quan M, Liu Z, Sun J, Shi S, Gong Y (2018) Positive effect of polymeric silane-based water repellent agents on the durability of superhydrophobic fabrics. Appl Surf Sci 450:492–501. https://doi.org/10.1016/j.apsusc.2018.04.204
18. Shang Q, Liu C, Zhou Y (2018) One-pot fabrication of robust hydrophobia and superoleophilic cotton fabrics for effective oil-water separation. J Coat Technol Res 15:65–75. https://doi.org/10.1007/s11998-017-9947-0
19. Stolz A, Le Floch S, Reinert L, Ramos SMM, Tuaillon-Combes J, Soneda Y, Chaudet P, Baillis D, Blanchard N, Duclaux L, Saint Miguel A (2016) Melamine-derived carbon sponges for oil-water separation. Carbon N Y 107:198–208. https://doi.org/10.1016/j.carbon.2016.05.05
20. Liang S, Neisius NM, Gaan S (2013) Recent developments in flame retardant polymeric coatings. Prog Org Coat 76:1642–1665. https://doi.org/10.1016/j.porgcoat.2013.07.014
21. Guido E, Alongi J, Colleoni C, Di Blasio A, Carosio F, Verelst M, Malucelli G, Rosace G (2013) Thermal stability and flame retardancy of polyester fabrics sol-gel treated in the presence of boehmite nanoparticles. Polym Degrad Stab 98:1609–1616. https://doi.org/10.1002/app.32954
22. Kowalczyk D, Brzezi´nski S, Kami´nska I (2015) Multifunctional bioactive and improving the performance durability nanocoatings for finishing PET/CO woven fabrics by the sol-gel method. J Alloy Compd 649:387–393. https://doi.org/10.1016/j.jallcom.2015.06.236
23. Foksowicz-Flaczyk J, Walentowska J, Przybylak M, Maciejewski H (2016) Multifunctional durable properties of textile materials modified by biocidal agents in the sol-gel process. Surf Coat Technol 304:160–166. https://doi.org/10.1016/j.surfcoat.2016.06.062
24. Dadvar S, Tavanai H, Dadvar H, Morshed M, Ghodsi FE (2011) UV-protection and photocatalytic properties of electrospun polyacrylonitrile nanofibrous mats coated with TiO2 nanofilm via sol-gel. J Sol Gel Sci Technol 59:269–275. https://doi.org/10.1007/s10971-011-2495-7
25. Brzezi´nski S, Kowalczyk D, Borak B, Jasiorski M, Tracz A (2011) Nanocoat finishing of polyester/cotton fabrics by the sol-gel method to improve their wear resistance. Fibres Text East Eur 6:83–88
26. Fouda MM, Wittke R, Knittel D, Schollmeyer E (2009) Use of chitosan/polyamine biopolymers based cotton as a model system to prepare antimicrobial wound dressing. Int J Diabetes Mellit 1:61–64. https://doi.org/10.1016/j.ijdm.2009.05.005
27. Haufe H, Thron A, Fiedler D, Mahltig B, Böttcher H (2005) Biocidal nanosol coatings. Surf Coat Int Part B Coat Trans 88:55–60. https://doi.org/10.1007/BF02699708
28. Chen G, Haase H, Mahltig B (2019) Chitosan-modified silica sol applications for the treatment of textile fabrics: A view on hydrophilic, antistatic and antimicrobial properties. J Sol Gel Sci Technol 91:461–470. https://doi.org/10.1007/s10971-019-05046-8

29. Abdel-Halim ES, Abdel-Mohdy FA, Al-Deyab SS, El-Newehy MH (2010) Chitosan and monochlorotriazinyl-β-cyclodextrin finishes improve antistatic properties of cotton/polyester blend and polyester fabrics. Carbohydr Polym 82:202–208, https://doi.org/10.1016/j.carbpol.2010.04.077
30. Ferrero F, Periolatto M (2017) Chitosan Coating on Textile Fibers for Functional Properties. In Thakur VK, Thakur MK, Kessler MR, Handbook of Composites from Renewable Materials, https://doi.org/10.1002/9781119441632.ch69
31. Ferrero F, Periolatto M, Ferrario S (2015) Sustainable antimicrobial finishing of cotton fabrics by chitosan UV-grafting: from laboratory experiments to semi industrial scale-up. J Clean Prod 96:244–252. https://doi.org/10.1016/j.jclepro.2013.12.044
32. Orsi G, De Maria C, Montemurro F, Chauhan VM, Aylott JW, Vozzi G (2015) Combinig inkject printing and sol-gel chemistry for making pH-sensitive surfaces. Curr Top Med Chem 15:271–278. https://doi.org/10.2174/1568026614666141229114738
33. Gvishi R, Sokolov I (2020) 3D sol–gel printing and sol–gel bonding for fabrication of macro- and micro/nano-structured photonic devices. J Sol Gel Sci Technol 95635–95648, https://doi.org/10.1007/s10971-020-05270-7
34. Derby B (2010) Inkjet printing of functional and structural materials: fluid property requirements, feature stability and resolution. Annu Rev Mat Res 40:395–414. https://doi.org/10.1146/annurev-matsci-070909-104502
35. Butt MA (2022) Thin-film coating methods: a successful marriage, of high-quality and cost-effectiveness—a brief exploration. Coatings 12:1115–1136
36. Jang D, Kim D, Moon J (2009) Influence of fluid physical properties on ink-jet printability. Langmuir 25:2629–2635. https://doi.org/10.1021/la900059m
37. Taurino R, Cannio M, Boccaccini DN, Bondioli MMF (2023) Preliminary study on the design of superhydrophobic surface by 3D inkjet printing of a sol-gel solution. J Sol Gel Sci Technol 108:368–376. https://doi.org/10.1007/s10971-023-06193-9
38. Bonet-Aracil M, Bou-Belda E, Gisbert-Payá J, Ibañez F (2019) In situ test: cotton sheets against mosquito bites in India. Cellulose 26:4655–4663. https://doi.org/10.1007/s10570-019-02395-z
39. Zhang S, Demir B, Ren X, Worley SD, Broughton RM, Huang TS (2019) Synthesis of Antibacterial N-halamine acryl acid copolymers and their application onto cotton. J Appl Polym Sci 136:1–8. https://doi.org/10.1002/app.47426
40. Mazzon G, Zahid M, Heredia-Guerrero JA, Balliana E, Zendri E, Athanassiou A, Bayer IS (2019) Hydrophobic treatment of woven cotton fabrics with polyurethane modified aminosilicone emulsions. Appl Surf Sci 490:331–342, https://doi.org/10.1016/j.apsusc.2019.06.069
41. Rinaudo M (2006) Chitin and chitosan: Properties and applications. Prog Polym Sci 31:603–632. https://doi.org/10.1016/j.progpolymsci.2006.06.001
42. Yang M, Liu W, Jiang C, Xie Y, Shi H, Zhang F, Wang Z (2019) Facile construction of robust superhydrophobic cotton textiles for effective UV protection, self-cleaning and oil-water separation. Colloids Surf A Physicochem Eng Asp 570:172–181. https://doi.org/10.1016/j.colsurfa.2019.03.024
43. Ravi LMP (2019) Enhanced adsorption capacity of designed bentonite and alginate beads for the effective removal of methylene blue. Appl Clay Sci 169:102–111. https://doi.org/10.1016/j.clay.2018.12.019
44. Liu S, Zhang Q, Gou S, Zhang L, Wang Z (2021) Esterification of cellulose using carboxylic acid-based deep eutectic solvents to produce high-yield cellulose nanofibers. Carbohydr Polym 251:117018. https://doi.org/10.1016/j.carbpol.2020.117018
45. Smitha S, Shajesh P, Mukundan P, Warrier KGK (2008) Sol-gel synthesis of biocompatible silica-chitosan hybrids and hydrophobic coatings. J Mater Sci Res 23:2053–2060. https://doi.org/10.1557/JMR.2008.0271
46. Ellerbrock R, Stein M, Schaller J (2022) Comparing amorphous silica, short-range-ordered silicates and silicic acid species by FTIR. Sci Rep 12:11708. https://doi.org/10.1038/s41598-022-15882-4
47. Benmokhtar S, Jazoulia AEL, Chaminade JP, Gravereau P, Menetrier M, Bouree F (2007) New process of preparation, structure, and physicochemical investigations of the new titanyl phosphate $Ti_2O(H_2O)(PO_4)(_2)$. J Solid State Chem 180:2713–2722. https://doi.org/10.1016/j.jssc.2007.07.028
48. Li YS, Wright PB, Puritt R, Tran T (2004) Vibrational spectroscopic studies of vinyltriethoxysilane sol–gel and its coating. Spectrochim Acta A Mol Biomol 60:2759–2766. https://doi.org/10.1016/j.saa.2003.12.047
49. Beckford S, Langston N, Zou M, Wei R (2011) Fabrication of durable hydrophobic surfaces through surface texturing. Appl Surf Sci 257:5688–5693. https://doi.org/10.1016/j.apsusc.2011.01.074
50. Taurino R, Bolelli G, Messi P, Iseppi R, Borgioli F, Galvanetto E, Caporali S (2024) Investigation of chemical, physical and mechanical properties of hybrid chitosan-silica based coatings for aluminium substrate. Surf Coat Tech 493:131265. https://doi.org/10.1016/j.surfcoat.2024.131265
51. Papamichael I, Voukkali I, Economou F, Liscio MC, Sospiro P, Naddeo V, Zorpas AA (2024) Investigation of customer behavior regarding circular fashion. Sustain Chem Pharm 41:101675. https://doi.org/10.1016/j.scp.2024.101675
52. Mitchell A, Spencer M, Edmiston C (2015) Role of healthcare apparel and other healthcare textiles in the transmission of pathogens: a review of the literature. J Hosp Infect 90:285–292. https://doi.org/10.1016/j.jhin.2015.02.017
53. Nilsen-Nygaard J, Strand SP, Vårum KM, Draget KI, Nordgård CT (2015) Chitosan: Gels and Interfacial Properties. Polymers 7:552–579. https://doi.org/10.3390/polym7030552
54. Fu J, Yanga F, Guo Z (2018) New The chitosan hydrogels: from structure to function. N J Chem 42:17162–17180. https://doi.org/10.1039/C8NJ03482F
55. Wang C, Yang H, Chen F, Peng L, Gao H-F, Zhao L-P (2018) Influences of VTMS/$SiO_2$ ratios on the contact angle and morphology of modified super-hydrophobic silicon dioxide material by vinyl trimethoxy silane, Results Phys 10891–10902, https://doi.org/10.1016/j.rinp.2018.08.007
56. Bonnar MP, Burnside BM, Christie J, Sceal EJ, Troupe CE, Wilson JIB (1999) Hydrophobic Coatings from Plasma Polymerized Vinyltrimethylsilane. Chem Vap Depos 5:117–125
57. Manatunga DC, de Silva RM, de Silva KMN (2015) Double layer approach to create durable superhydrophobicity on cotton fabric using nano silica and auxiliary non fluorinated materials. Appl Surf Sci 360:777–788. https://doi.org/10.1016/j.apsusc.2015.11.068(2016)
58. He X, Zhou W (2024) Hydrophobic modification and durability protection of cotton garment fabric surfaces by graphene oxide/PGMA composite coatings. Sci Rep 14:30174. https://doi.org/10.1038/s41598-024-71736-1
59. Mahbubul-Bashar M, Khan MA (2013) An overview on surface modification of cotton fiber for apparel use. J Polym Environ 21:181–190, https://doi.org/10.1007/s10924-012-0476-8(2013).
60. Zhou Z, Ruiz Cantu L, Chen X, Alexander MR, Roberts CJ, Hague R, Tuck C, Irvine D, Wildman R (2019) High-throughput characterization of fluid properties to predict droplet ejection for three-dimensional inkjet printing formulations. Addit Manuf 29:100792. https://doi.org/10.1016/j.addma.2019.100792